MODELING EFFECTS ON TRANSIENT BEHAVIOR OF SYNCHRONOUS MACHINES

Sebastião E.M. de Oliveira
Centro de Pesquisas de Energia Elétrica - CEPEL
P.O.Box 2754, Rio de Janeiro, 20001, BRAZIL

ABSTRACT

In the present paper the synchronous generator transient behavior is analized for some modes of operation. More detailed modeling is considered in order to illustrate both effects of the non-equal mutual coupling between direct-axis windings and of a higher order rotor representation for the direct and quadrature axes.

Data derived from standstill response tests in a 25 MVA, 6.9 kV, 48 poles, 2092 A, 150 rpm, 0.9 power factor salient-pole synchronous generator are used to simulate the machine behavior under modes of transient disturbances like simultaneous three-phase short-circuit, direct axis load rejection and quadrature axis load rejection. Model structures and associated data utilized in the simulations incorporate second and third-order effects on direct axis and first and second-order effects on quadrature axis.

Keywords: synchronous machine modeling, transient behavior, three-phase short-circuit, direct-axis load rejection, quadrature-axis load rejection.

1.0 - INTRODUCTION

Proper modeling of synchronous machines is essential for an improved evaluation of the influence of their voltage control and rotor angle oscillations on power system transient performance. Two factors are extremely important if more consistent representation is to be achieved: a definition of the model structure valid for the frequency range of interest and calculation of the parameters associated with the established representation.

Good and reliable synchronous machine models are required therefore for analyzing and simulating the performance of power systems. A methodology not yet broadly, although receiving increased attention nowadays, is based on the standstill frequency response (SSFR) tests, an interesting alternative to the usual simultaneous three-phase short-circuit test for obtaining synchronous machine parameters. SSFR tests allow definition of the number of equivalent rotor windings for proper modeling rotor effects and provide complete data for both direct axis and quadrature axis equivalent circuits.

While several computational programs only allow a first or second order representation for the electromagnetic effects on turbogenerators and hydrogenerators' direct and quadrature axis, results of measurements from the standstill frequency response tests can be used in the task of defining higher order models. Generally, the need for higher order models may appear when it is desired to represent certain transient phenomena involving a wider frequency range.

Second order models show appropriate performance in simulating dynamic phenomena in the frequency range from DC to 6 Hz as seen from field circuit axis and, therefore, can be utilized with expectation of good results for simulating low frequency transient phenomena. The data necessary for use in conjunction with second order models have been traditionally obtained from generator manufacturers and taken from oscillograms of sudden simultaneous three-phase short-circuit tests.

Other types of tests nowadays are receiving increased attention, because there is a need to represent better the transient effects related to machine quadrature axis and also because frequency components above 10 Hz are of interest for analysis of other phenomena like subsynchronous resonance. Load rejection tests and standstill frequency response (SSFR) tests, for instance, are specially interesting on this matter of quadrature axis modeling. SSFR tests are still appropriate for model structure analysis and for higher order representations by equivalent circuits.

The present paper analyses the effects of differences in the synchronous generator model representation on the different modes of machine transient behavior, for various degrees of modeling complexity. Computer simulation traces for machine voltages and currents following disturbances like simultaneous three-phase short-circuit, direct-axis load rejection and quadrature axis load rejection are presented.

Model structures and associated data utilized in the simulations incorporate second and third-order effects on direct axis and first and second-order effects on quadrature axis. Data used were derived from SSFR

tests in a 25 MVA, 6.9 kV, 48 poles, 2092 A, 150 rpm, 0.9 power factor salient-pole synchronous generator.

2.0 - SYNCHRONOUS MACHINE PARAMETERS BY STANDSTILL FREQUENCY RESPONSE TESTS

The standstill frequency response tests are carried out independently for direct and quadrature axis. The Standard IEEE 115-A recommends three different sets of test measurements: a first set to obtain the quadrature axis operational impedance $X_q(s)$, a second one to be carried out with the field circuit short-circuited for identifying both the direct axis operational impedance $X_d(s)$ and the transfer function field-armature $s.G(s)$ and a third set of test measurements with the field open.

In addition to these tests, we also performed a set of measurements with voltage applied to the field circuit and with the armature open. From the low frequency range of this set, the effective field resistance value may be checked. These measurements and the others were carried out in a frequency range from 0.001 to 100 Hz. Stator currents during the test were limited to 12 A, which corresponds to 0.6% of the rated value.

Figure 1 indicates the connections to the stator phase windings, the rotor field circuit, the power supply, the signal generator and the digital oscilloscope for one set of measurements.

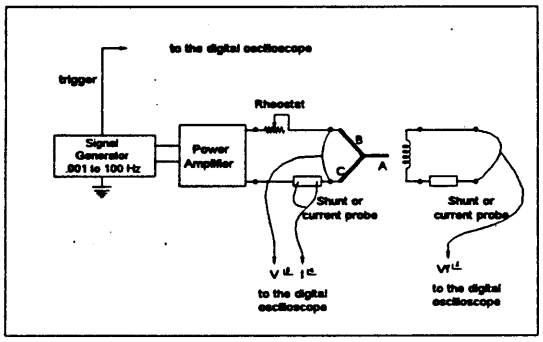

Figure 1 - Connections for the main SSFR tests. Third set of measurements. Voltage applied to armature. Field winding open. $I_{arm} = 12A, \ I_f = 0$

Before the main d-axis or q-axis test measurements, it is necessary to align the axis direction in the rotor with the expected direction for the armature reaction in the stator. For direct axis alignment we used the same scheme for phase connections indicated in Figure 2 as recommended by Standard IEEE 115-A. The direct axis positioning from 30 electrical degrees lagging phase B axis in Figure 2 occurs when the fundamental component of the field circuit induced voltage is annulled. This component was derived from signal FFT of the field circuit induced voltage transferred to the digital oscilloscope.

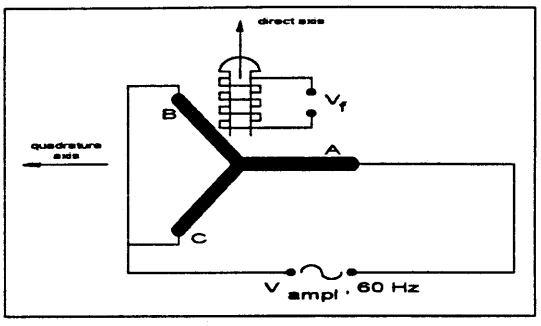

Figure 2 - Armature circuit supplying scheme for positioning the direct axis

3. - MODEL STRUCTURES FOR SYNCHRONOUS MACHINE REPRESENTATION

Synchronous machine representation allows rotor effects modeling by any number of equivalent circuits. Naturally higher order model structures represented by a large number of equivalent circuits may lead to a more precise representation. Other complex effects such as that related to the differences of mutual coupling between the direct axis windings can also be incorporated to the modeling without changes in the form of the mathematical representation by transfer functions.

Regardless of the number of circuits selected for machine rotor representation in the direct and quadrature axis, but taking into account zero rotor speed during the SSFR tests, we may write in the complex domain:

$$V_d(s) = Z_d(s) \, . \, I_d(s) + s \, . \, G(s) \, . \, V_f(s) \quad (1)$$

$$I_f(s) = s \, . \, G(s) \, . \, I_d(s) + Y_{f0}(s) \, . \, V_f(s) \quad (2)$$

$$V_q(s) = Z_q(s) \, . \, I_q(s) \quad (3)$$

V_f and I_f are terminal voltage and current in the field circuit. V_d, V_q, I_d and I_q are the d-axis and q-axis components of stator phase voltages and currents.

If SSFR tests are carried out with armature current open, then $I_d(s) = 0$ in equations 1 and 2 and we are able to define the frequency response curves for $s.G(s)$ or $Y_{fo}(s)$ from the test measurements. When the field circuit is short-circuited, then $V_f(s) = 0$, $Z_d(s)$ and $s.G(s)$ may also be extracted from the set of test measurements. From identification techniques then it is possible to derive the machine parameters related to a certain model structure.

Tables 1 in appendix lists the parameters related to the d-axis model structures that now will be mentioned and that were derived from SSFR test carried out in a 6.9 kV, 25 MVA machine. Figure 3 shows the equivalent

circuit for d-axis representation considering third-order rotor modeling but taking into account the non-equal mutual inductances in d-axis. The differential reactances presented in Table 1 are shown in Figure 3. Table 2 presents machine data derived from the SSFR set of measurements related to the q-axis test. First-order and second-order rotor modeling were derived for the quadrature axis.

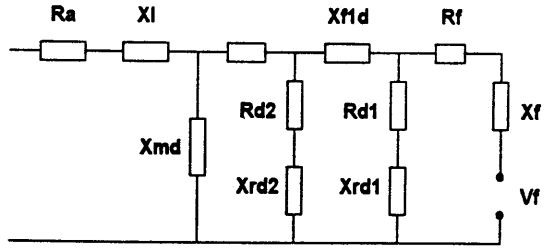

Figure 3 - Direct-axis third-order equivalent circuit including the effect of non-equal mutual couplings.

4. - THREE-PHASE SHORT-CIRCUIT TRANSIENTS

In order to observe the modeling effects on synchronous machine transient behavior, a simultaneous three-phase short-circuit in an unloaded machine was simulated. Pre-fault terminal voltage equal to 0.3332 pu was considered in order to produce phase currents presenting nearly nominal subtransient d-axis fundamental component. Figures 4 to 11 show some curves related to this disturbance. The effect of d-axis rotor modeling by one or two damper windings (second or third-order d-axis rotor modeling) and of q-axis modeling by one or two damper windings (first or second-order q-axis rotor modeling) can be observed in Figures 4, 6 and 8 to 11. The effect of modeling the non-equal mutual couplings among d-axis windings is only observed in Figures 5 and 7 on machine field current. Stator variables do not present differences when non-equal mutual coupling is included in modeling.

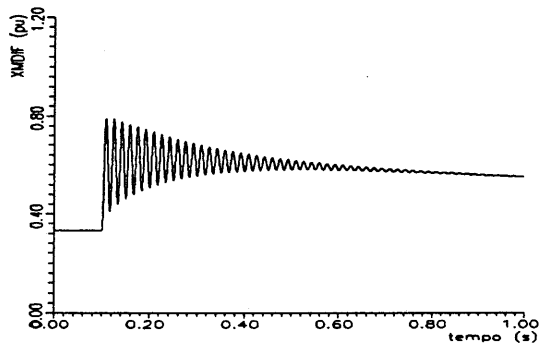

Fig.4 - Field current during a three-phase short-circuit in an initially unloaded machine. Third-order d-axis and second-order q-axis rotor representation. Equal mutual coupling in d-axis.

As a general conclusion, field current presents large deviations when salient-pole synchronous machine modeling incorporates the effect of non-equal mutual coupling among windings in direct axis.

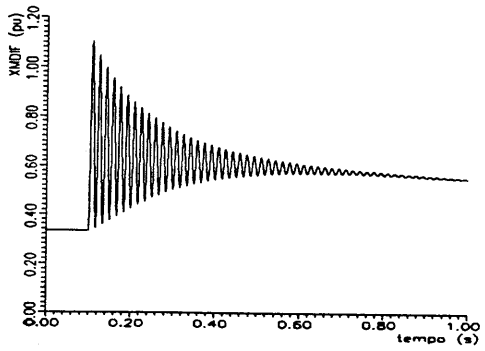

Fig.5 - Field current during a three-phase short-circuit in an initially unloaded machine. Third-order d-axis and second-order q-axis rotor representation. Non-equal mutual coupling in d-axis.

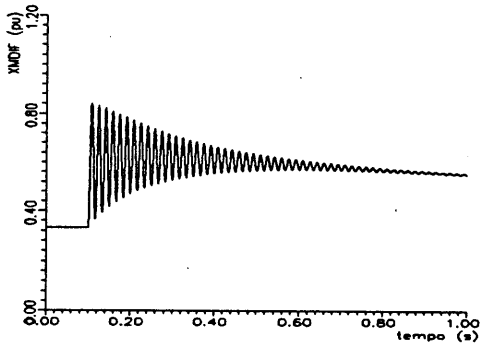

Fig.6 - Field current during a three-phase short-circuit in an initially unloaded machine. Second-order d-axis and first-order q-axis rotor representation. Equal mutual coupling in d-axis.

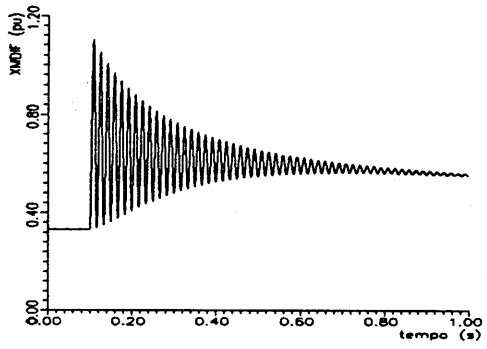

Fig.7 - Field current during a three-phase short-circuit in an initially unloaded machine. Second-order d-axis and first-order q-axis rotor representation. Non-equal mutual coupling in d-axis.

Phase currents can be practically divided into a DC or unidirectional component and an alternating component of fundamental frequency. A small second harmonic component is also present but in most cases it is of negligible amplitude. The unidirectional component in Figures 8 and 9 completely moves the line drawn half-way between the envelope curves away from zero value.

Since higher order modeling leads generally to lower subtransient reactances in both d and q axes, the 60 Hz component in Figure 8 is slightly larger than in Figure 9. The same effect is observed in Figures 10 and 11 with respect to the d-axis component of the stator current. The 60 Hz component has initial amplitude slightly larger in Figures 10 than in Figure 11 since it is inversely proportional to the d-axis subtransient reactance.

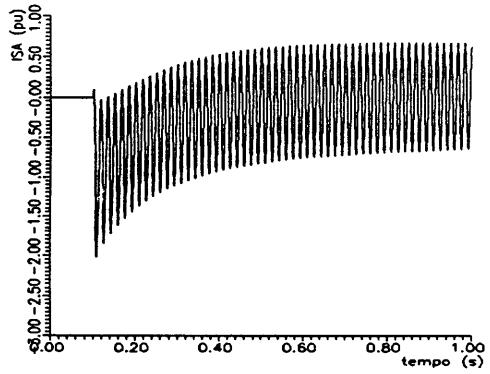

Fig. 8 - Phase A stator current during a three-phase short-circuit in an initially unloaded machine. Third-order d-axis and second-order q-axis rotor representation.

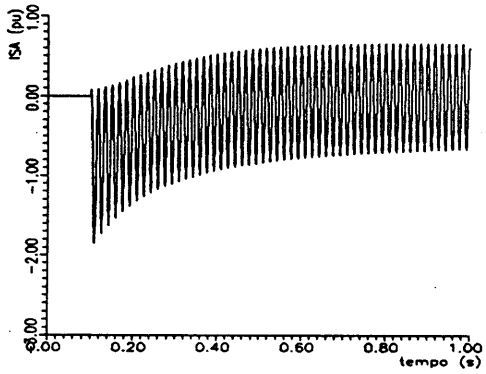

Fig. 9- Phase-A stator current during a three-phase short-circuit in an initially unloaded machine. Second-order d-axis and first-order q-axis rotor modeling

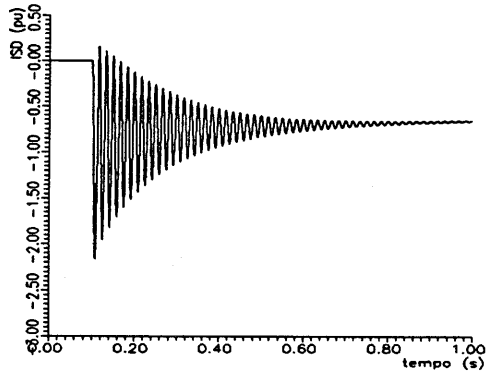

Fig.10- D-axis stator current during a three-phase short-circuit in an initially unloaded machine. Third-order d-axis and second-order q-axis rotor representation.

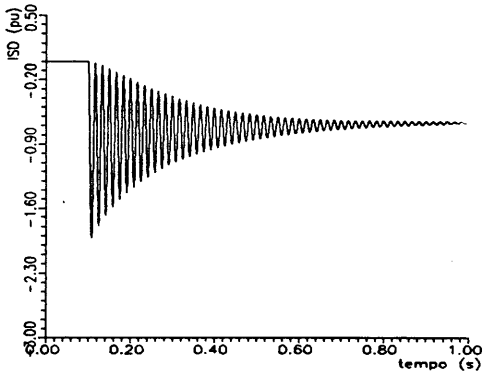

Fig.11- D-axis stator current during a three-phase short-circuit in an initially unloaded machine. Second-order d-axis and first-order q-axis rotor representation.

5 - TRANSIENT BEHAVIOR FOLLOWING LOAD REJECTION

5.1 - D-axis load rejection

A second disturbance considered in this paper was a load rejection of an initially unloaded machine, but receiving reactive power of 0.6 pu from the power system. Rated terminal voltage was established before the rejection. P = 0, Q = -0.6 pu, Vt = 1.0 pu.

Figures 12 to 15 shows field current d[illegible] following d-axis rejection. The difference on d[illegible] at zero time characterizes both effects of non-equal mutual coupling and higher order rotor representation. Deviations on field current at zero time are much larger when non-equal mutual coupling is represented (Figures 13 and 15). For lower order representation as indicated in Figures 14 and 15, an additional increasing on field current deviation is also observed.

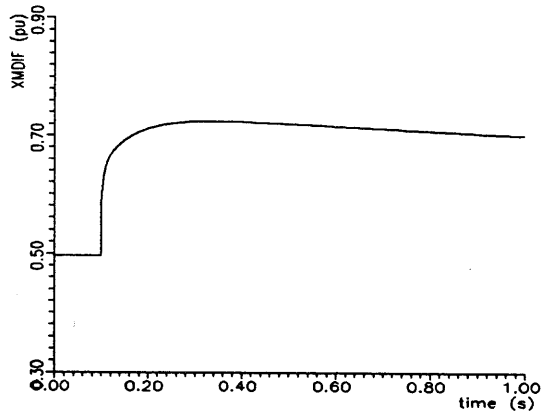

Figure 12 - Field current during a purely reactive load rejection. Third-order d-axis representation. Equal mutual coupling in d-axis

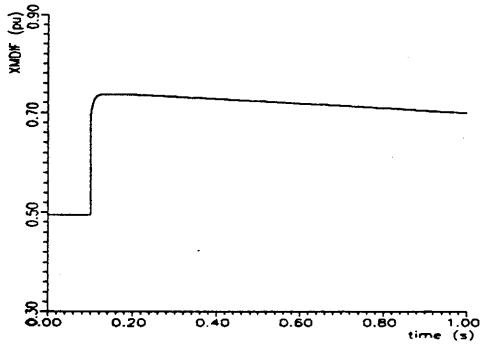

Figure 13 - Field current during a purely reactive load rejection . Third-order d-axis representation. Non-equal mutual coupling in d-axis

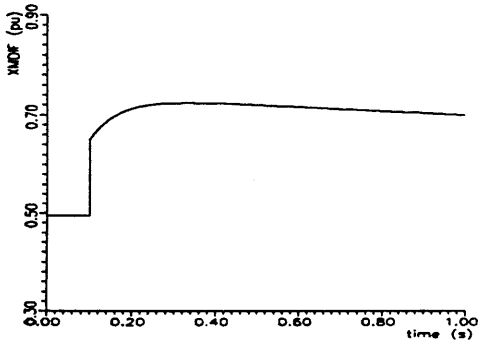

Figure 14 - Field current during a purely reactive load rejection. Second-order d-axis representation. Equal mutual coupling in d-axis

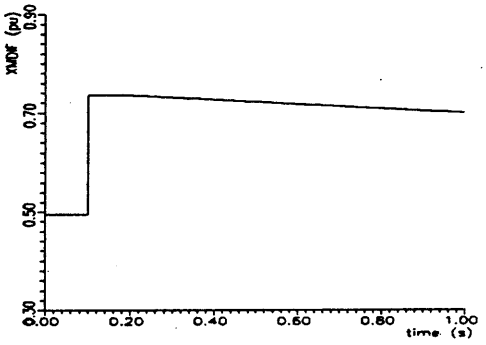

Figure 15 - Field current during a purely reactive load rejection. Second-order d-axis representation. Non-equal mutual coupling in d-axis

Figures 16 and 17 show curves for the q-axis component of the stator voltage. Again zero time deviation on this variable is slightly larger when the lower order rotor modeling is considered (Figure 17).

5.2 - Q-axis load rejection

Another disturbance is considered in this section. Now a load rejection of an initially loaded machine is simulated but in such a way that flux changes only occur in the q-axis. By properly defining the amount of reactive power the machine is absorbing from the power system, the armature reaction can be aligned to the q axis before the disturbance. For P = 0.7 pu and Vt = 1.0 pu, reactive power for purely quadrature axis rejection was found equal to Q = - 0.3103 pu.

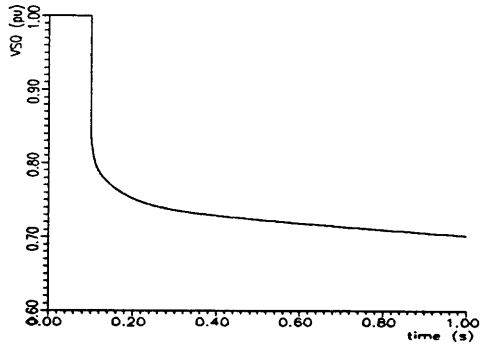

Figure 16 - Q-axis stator voltage during a purely reactive load rejection. Third-order d-axis representation.

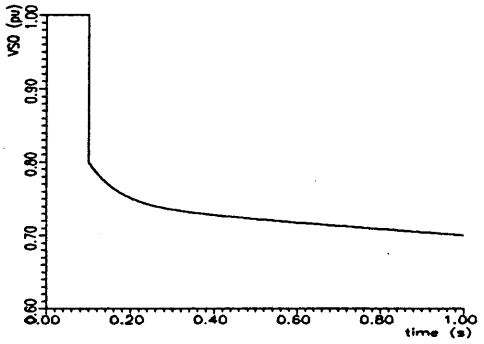

Figure 17 - Q-axis stator voltage during a purely reactive load rejection . Second-order d-axis representation.

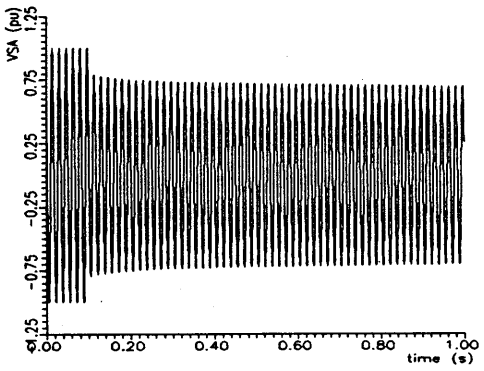

Figure 18 - Phase A stator voltage during a purely reactive load rejection. Second-order d-axis rotor representation.

Field current deviations are not presented in this case because they are practically annulled when armature reaction does not present d-axis component. In fact this condition was used in order to verify if armature reaction was really in q-axis before the rejection.

Figures 19 and 20 show the direct-axis component of stator voltage following load rejection. Again we observe a slightly larger zero time deviation when a first order rotor modeling is considered for the quadrature axis.

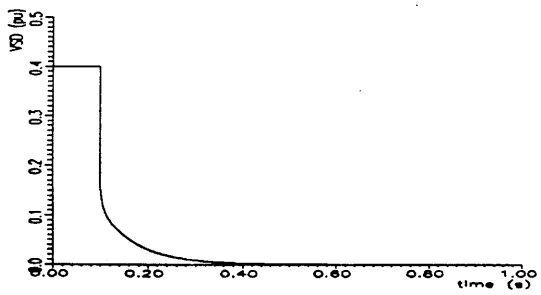

Figure 19 - D-axis stator voltage during a real and reactive load rejection. Second-order q-axis rotor modeling.

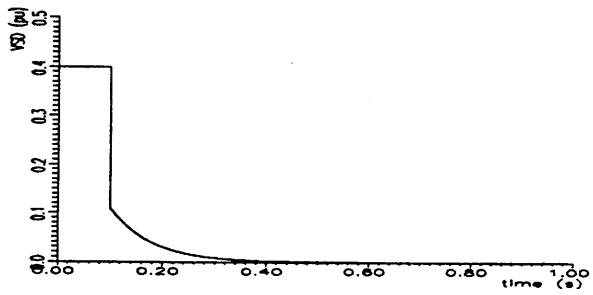

Figure 20 - D-axis stator voltage during a real and reactive load rejection. First-order q-axis rotor modeling.

6 - CONCLUSIONS

The paper presents results of computer traces for the variables that better describes synchronous machine behavior under some disturbances, such that the effect of different model structures is emphasized.

Data for the structures were derived from standstill frequency response tests. Since higher order modeling generally leads to reproduction of frequency response test data in a large frequency range, subtransient reactances tend therefore to present lower values.

The effects of such reduce subtransient reactances as well as those related to the non-equal mutual couplings among d-axis windings on the transients are demonstrated. Differences on the computer traces did appear only during the subtransient periods related to rotor and armature time constants. Therefore, carefully analysis of the subtransient period is necessary in order to better capture the zero time changes and characterize the model structure. Only negligible differences on the transient components were observed.

It is recommendable therefore that identification procedures should be considered in order to decide which model and related parameters better represent the machine behavior under transient and steady-state operation.

7 - REFERENCES

[1] - IEEE Standard Procedure for Obtaining Synchronous Machine Parameters from Standstill Frequency Response Testing, IEEE Std. 115A, 1987.

[2] - Ruche, P.A., Brock, G.J., Hannet, L.N., Willis, J.R., Test and Simulation of Network Dynamic Response using SSFR and RTDR Derived Synchronous Machine Models, IEEE Trans. on Energy Conversion, vo. 5, no.1, March 1990.

8. - APPENDIX

	third order model	second order model	third order model	second order model
Xd	.8400	.8400	.8400	.8400
Xl	.1600	.1600	.1600	.1600
X'd	.4328	.4329	.4328	.4329
X"d	.3412	.3332	.3412	.3332
X'"d	.2632		.2632	
T'do	5.0452	5.0429	5.0452	5.0429
T"do	.06879	.07115	.06879	.07115
T"'do	.006389		.006389	
Rf	.6053	.6046	.5943	.5939
Xf	.4610	.4603	1.0512	1.0280
Rd1	.02977	.02751	.1570	.1468
Xrd1	.5129	.4693	4.1163	3.8463
Rd2	.1772		.4525	
Xrd2	.2433		.8396	
Xf1d			-.4655	-.5788
Xf12d			-.1362	

Table 1 - Reactances, time constants and parameters for third and second-order d-axis machine modeling derived by SSFR tests. columns 2 and 3 (equal mutual coupling), colums 4 and 5 (non-equal mutual coupling)

	second order model	first order model
Xq	0.5225	0.5225
X'q	0.3798	
X"q	0.3210	0.3781
T'qo	0.07653	
T"qo	0.00543	0.07653
Rq1	0.03294	0.03154
Xq1	0.5750	0.5475
Rq2	0.3884	
Xrq2	0.5835	

Table 2 - Reactances, time constants and parameters for first and second-order q-axis machine modeling derived by SSFR tests.